Velocity analysis in the presence of amplitude variation

Debashish Sarkar*, Bob Baumel† and Ken Larner*

* *Center for Wave Phenomena, Department of Geophysics, Colorado School of Mines*
† *Conoco Inc., Ponca City, OK*

ABSTRACT

Conventional semblance velocity analysis (Taner and Koehler, 1969) is equivalent to modeling prestack seismic data with events that have hyperbolic moveout but no amplitude variation with offset (AVO). As a result of its assumption that amplitude is independent of offset, this method may not perform well for events with strong AVO, especially for events with polarity reversals at large offset, such as reflections from tops of some class 1 and class 2 sands.

To account for AVO, the semblance method can be extended by modeling the data with events that have not only hyperbolic moveout, but also amplitude variation, expressed by AVO intercept and gradient (i.e., the Shuey approximation). However, due to the extra degrees of freedom introduced by modeling AVO with the AVO-sensitive semblance, resolution of the estimated velocities tends to decrease. This is because the data can be modeled acceptably with a combination of incorrect velocities and incorrect AVO behavior, resulting in large values of AVO-sensitive semblance even at the wrong velocities.

One solution to this problem is a hybrid method that combines the AVO-sensitive semblance and ordinary semblance methods through use of a regularization parameter. Here, we follow a somewhat different approach. We also use the Shuey equation to describe the amplitude variation and, in addition, constrain the AVO parameters (intercept and gradient) to be linearly related. With this constraint we can preserve velocity resolution, without the use of a regularization parameter, while improving the quality of velocity analysis in the presence of amplitude variation with offset. Results for a number of tests show the modified semblance approach to be somewhat more robust in the presence of noise than conventional semblance and much more accurate when polarity changes with offset.

Introduction

Corcoran (1989) and Sarkar, Lamb and Castagna (1999) have shown that the semblance measure of Taner and Koehler (1969) is based on the implicit assumption that the wavelet does not vary with offset. Success with that measure lies in its model simplicity, which makes the procedure robust against noise. The conventional semblance measure (here, we shall call it "traditional semblance"), evaluated at zero-offset time t_o is defined as

$$S(v,t_o) = \frac{\sum_{t_1}\left(\sum_x D_v(t_1,x)\right)^2}{N\sum_{t_1}\sum_x D_v^2(t_1,x)}, \qquad (1)$$

where $D_v(t_1,x) = D[t_v(t_1,x),x]$, with $t_v(t_1,x) = \sqrt{t_1^2 + \frac{x^2}{v^2}}$; t_1 are zero-offset times within a window centered at t_o; and N is the number of traces. D_v represents the data moveout-corrected with velocity v, and D represents the data without NMO correction. Due to the assumption that amplitude is independent of offset, the measure is degraded in the presence of large amplitude variations. In such cases the value of S decreases. In the presence of polarity reversals at large offset, such as happens for some reflections from the tops of class 1 and class 2 sands, the method yields highly erroneous results.

Recently other methods have been developed which tackle the problem of amplitude variation and polarity reversal to a certain extent. The differential semblance method (e.g., Symes and Kern, 1994) works by taking the difference of adjacent traces. The objective function is such that it eliminates secondary maxima and produces a broad primary maximum. This indicates its poor velocity resolution. Because it takes the difference of traces

for neighboring offsets, amplitude variation with offset has little influence on the semblance curves. However, due to the broad semblance curves obtained through this method, it may not be suitable for generating standard semblance panels. Eigenvalue methods (e.g., Biondi and Kostov, 1989; Key and Smithson, 1990), which exploit the fact that the signal covariance matrix is of low rank in the absence of noise, easily incorporate AVO, even for complex variations. They can also tackle multiple conflicting events (Biondi and Kostov, 1989). Their vulnerability to noise, however, is not well known, and they are more expensive than other commonly used velocity analysis procedures (the dominant cost is in the computation of the eigenvalues, which is proportional to m^3, where m is the dimension of the covariance matrix).

To generalize traditional semblance to events with large amplitude variation with offset, especially for events with polarity reversal, an amplitude-dependent function, such as that in Shuey (1985), can be incorporated in the semblance measure (Corcoran, 1989). This method successfully estimates velocities of seismic events that have not only large AVO but also polarity reversals. The increased number of parameters, however, results in the loss of velocity precision, especially when the range of incidence angles is small. To improve the estimation of velocities Sarkar (1999) suggested solving the problem as a mixed-determined problem (Menke, 1984) that incorporates the use of a regularization term. That formalism showed how one could obtain results varying from those of traditional semblance to those of an amplitude-dependent semblance by varying the regularization parameter. The user is required to choose a value for the regularization parameter — a task that is often difficult.

Here, we describe a method that does not require a regularization term and that preserves the good aspects of both traditional semblance and amplitude-dependent semblance, regardless of amplitude variation with offset.

AVO-sensitive semblance formalism

To incorporate amplitude variation with offset into velocity analysis, we first define the *generalized semblance* as

$$S_G(v,t_o) = 1 - \frac{\|M - D_v\|^2}{\|D_v\|^2}, \tag{2}$$

where, as before, v is a trial velocity and t_o is zero-offset time at the center of a semblance window. $D_v = D_v(t_1,x)$ is the data after moveout correction with velocity v, and $M = M(t_1,x)$ is a suitably parameterized model of the trace amplitudes in the moved-out data. The model parameters are obtained by minimizing $\|M - D_v\|^2$ or, equivalently, maximizing the generalized semblance. The vector norms include sums over all offsets and all zero-offset times within the semblance window.

The computation of the generalized semblance consists of three steps. In step one, we define the model function M as a linear combination of basis functions that describe the amplitude variation with offset. A particular case of such a function is the Shuey equation (Shuey, 1985), which describes the offset dependence of amplitude in terms of the angle of incidence at the reflector. For models that are not too complex, this angle can be estimated by ray tracing. In step two, we determine the coefficients of the model, M, such that the model is a least-squares fit to the data. This is achieved by setting the derivatives of equation (2) with respect to the model coefficients equal to zero and solving the resulting overdetermined, unconstrained least-squares problem. In the third step, we substitute M back into equation (2) to obtain the generalized semblance for each zero-offset time and trial stacking velocity. Since the model coefficients are estimated from the data, they are dependent on velocity, so the semblance measure is also velocity-dependent. The trial velocity that maximizes the semblance measure is taken as the stacking velocity.

The simplest parameterization for the model M in equation (2) is an offset-independent model; i.e., $M(t_1,x) = A(t_1)$. For this model, if N_t denotes the number of time samples in a semblance window, N_t parameters have to be estimated for each semblance window. Expanding equation (2) for a particular time t_1 we have

$$S_G(v,t_o) = 1 - \frac{\sum_x (A(t_1) - D_v(t_1,x))^2}{\sum_x D_v^2(t_1,x)}. \tag{3}$$

Taking derivatives with respect to $A(t_1)$ and setting them to zero gives

$$NA(t_1) = \sum_x D_v(t_1,x). \tag{4}$$

Thus, the optimal parameter values are given simply by the stack trace, $A(t_1) = \frac{1}{N}\sum_x D_v(t_1,x)$. When this expression is substituted into the generalized semblance [equation (2)] we get,

$$\begin{aligned} S_G(v,t_o) \quad = \quad & \frac{\sum_x \frac{2}{N} D_v(t_1,x) \sum_{x_1} D_v(t_1,x_1)}{\sum_x D_v^2(t_1,x)} \\ & - \frac{\sum_x \frac{1}{N^2} (\sum_{x_1} D_v(t_1,x_1))^2}{\sum_x D_v^2(t_1,x)}, \end{aligned} \tag{5}$$

or,

$$S_G(v,t_o) = \frac{\left(\sum_x D_v(t_1,x)\right)^2}{N\sum_x D_v^2(t_1,x)}, \tag{6}$$

which is just the traditional semblance [equation(1)] computed for a particular zero-offset time t_1. This result shows that traditional semblance is optimal when trace amplitude is independent of offset.

When amplitude variation is present, then the traditional semblance value decreases even in the absence of noise. For example, for three traces with amplitudes 1, 2 and 3, the traditional semblance would equal 0.86. If, however, all three values are identical, then the semblance value would equal 1. Thus, in the presence of amplitude variation, the traditional semblance value would be reduced, somewhat, relative to the level for background noise.

To account for AVO, we choose a model parameterization based on the Shuey (1985) simplification of the Zoeppritz equation, i.e.,

$$M(t_1, x) = A(t_1) + B(t_1) \sin^2 \theta_x, \tag{7}$$

where $\theta_x = \theta_x(t_1, v)$ is the angle of incidence at the reflector. This is the model used by both Corcoran (1989) and Sarkar, Lamb and Castagna (1999). Here, the model contains $2N_t$ parameters for each semblance window, namely, all of the $A(t_1)$ and $B(t_1)$ coefficients. For each time t_1 inside the semblance window centered on t_o and governed by trial velocity v, we estimate $A(t_1)$ and $B(t_1)$. These estimated coefficients are then substituted into equation (7), which is subsequently used to compute the generalized semblance, equation (2). This sequence of steps is then repeated for each trial velocity v. We shall call this approach in which the A and B parameters are estimated independently the "AB semblance" method.

Equation (7) models AVO behavior independently at each zero-offset time t_1. Unfortunately, this allows too much freedom to fit events with combinations of incorrect velocity and incorrect AVO, resulting in poor velocity resolution. To reduce the number of degrees of freedom, we constrain the relationship between AVO intercept and gradient within a wavelet. The amplitude at every point within a wavelet should be a scaled version of the amplitude at the peak of the wavelet. Assuming that the wavelet shape does not change with offset, the amplitude variation along any moveout curve with zero-offset time t_1 within a wavelet would be a scaled version of the amplitude variation with offset along the moveout trajectory traced out by the center of the wavelet. Thus, the ratio of the amplitude gradient to the zero-offset amplitude should be constant for all moveout curves within a wavelet. Since, we choose the semblance window length to approximate the length of the wavelet, we make the additional assumption that the window is centered on the reflection moveout trajectory of a single wavelet and that this ratio is constant over the semblance window; that is, we make the ratio $K = \frac{B(t_1)}{A(t_1)}$ constant throughout each semblance window. We finally assume that the semblance window contains just a single event or several events, all having identical AVO behavior. This set of assumptions leads to the model parameterization,

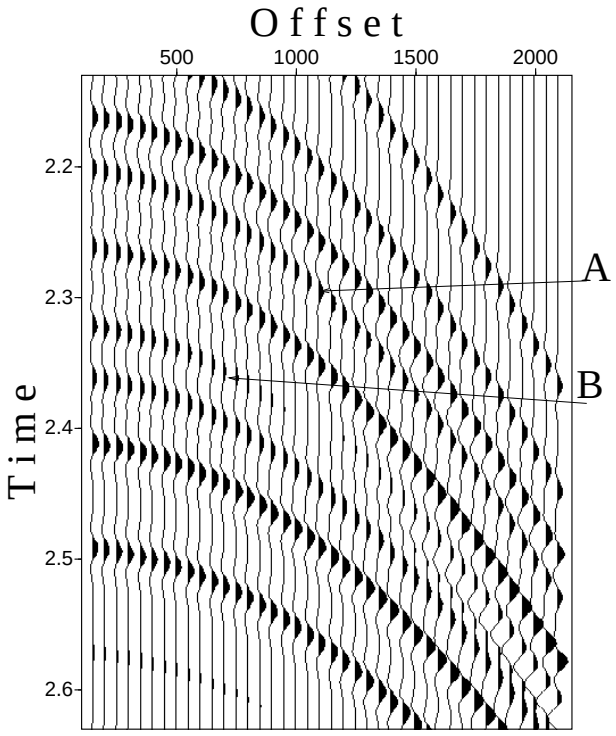

Figure 1. Synthetic CMP gather. Event A has no amplitude variation, and event B exhibits a polarity reversal. Semblance plots for velocity analysis on events A and B are shown in Figures 2 and 3.

$$M(t_1, x) = A(t_1)(1 + K \sin^2 \theta_x), \tag{8}$$

where K is fixed within each semblance window. This model in which the B parameters are constrained to being proportional to the A parameters contains only N_t+1 parameters for each semblance window. We refer to this approach as the "AK semblance" method. In it, we estimate coefficients $A(t_1)$ and K for each velocity and use the estimated coefficients to compute the model M in the generalized semblance S_G.

Tests with modeled data

Test 1: No noise; polarity reversal with offset

We applied the three methods — traditional semblance, AB semblance and AK semblance — to the synthetic common-midpoint (CMP) gather shown in Figure 1. First, we analyze two selected reflections — one with

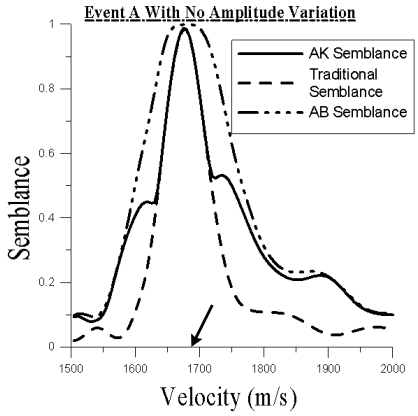

Figure 2. Semblance curves for event A (no amplitude variation). The correct stacking velocity (1685 m/s) is marked with an arrow.

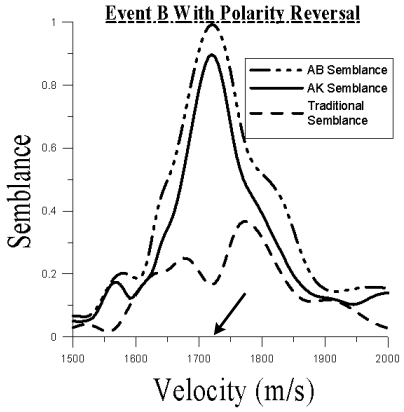

Figure 3. Semblance curves for event B (polarity reversal). The correct stacking velocity (1720 m/s) is marked with an arrow.

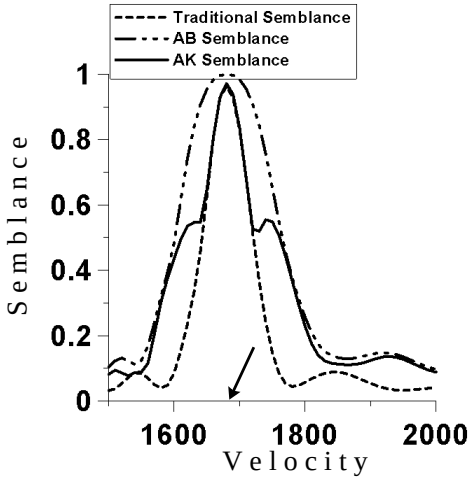

Figure 4. Semblance curves for event A computed for a computation window that is 13 ms earlier than the center of the event. In this and subsequent figures, units of velocity are in m/s.

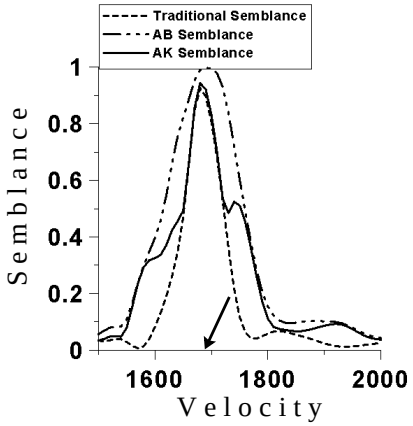

Figure 5. Semblance curves for event A computed for a computation window that is 13 ms later than the center of the event.

almost no variation of amplitude with offset (event A) and the other with a polarity reversal (event B) — with the velocity analysis performed on a window centered on each event. The semblance curves obtained by the three methods are shown in Figures 2 and 3. For the event with no amplitude variation with offset, all three methods have their maximum semblance value near the correct stacking velocity (1685 m/s). Of the three methods traditional semblance has the smallest width, indicative of its good velocity resolution, while AB semblance has the largest width, and thus the poorest velocity resolution. Traditional semblance has the best resolution because it allows for the fewest degrees of freedom, while AB semblance has poor resolution because it has the most degrees of freedom. The AK semblance overlaps that of the traditional semblance near the correct velocity (where performance is most important), but it jumps to approximate the AB semblance for velocities far from the correct one. Thus, in the presence of little or no amplitude variation with offset, the AK semblance measure matches the resolution and accuracy performance of traditional semblance without the need of a regularization parameter.

Figure 3 shows the performance of the different methods in the presence of a polarity reversal along a reflector. As expected, the traditional semblance method fails — in terms of velocity accuracy, resolution and

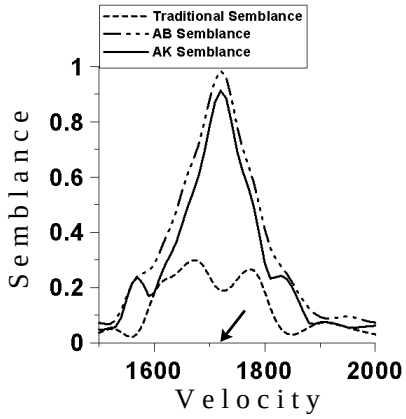

Figure 6. Semblance curves for event B computed for a computation window that is 13 ms earlier than the center of the event.

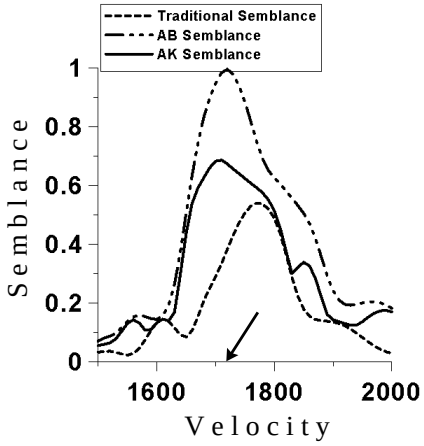

Figure 7. Semblance curves for event B computed for a computation window that is 13 ms later than the center of the event.

standout of the peak. This is because traditional semblance looks for events with constant amplitude with offset, which in the case of polarity reversals can be best approximated when a near-offset peak aligns with a side lobe of the same wavelet at far-offset. Near the correct velocity, the amplitudes cancel producing small semblance values. Hence, the wrong velocities will show the highest semblance. Both, the AB semblance and the AK semblance, however, peak near the correct stacking velocity, 1720 m/s, in Figure 3. The results in Figures 2 and 3 suggest that the AK semblance can provide a method for estimating velocities of both events with polarity reversal and those without any amplitude variation, while retaining the resolution of traditional semblance in the absence of amplitude variation with offset.

Test 2: No noise; window off center

In Figures 4-7, we compare the performances of the three methods when the velocity analysis is done on the same events shown in Figure 1 but with a zero-offset time that differs from that of the center of the wavelet. Figures 4 and 6 show semblance plots computed with a zero-offset time that is 13 ms earlier than the center of the wavelet (the dominant period of the wavelet is 50 ms and the window length is 52 ms), and Figures 5 and 7 show semblance plots computed at zero-offset time that is 13 ms later than the center of the wavelet. Comparing Figures 2, 4 and 5, first note that, for all three semblance methods, the semblance peak drifts with departure of the computation window from the center of the wavelet. This behavior is well known in traditional velocity analysis. Second, note that the peak AB semblance value stays near unity even as the window center moves away from the center of the wavelet, whereas the peak semblance values for the traditional and AK semblance approaches decrease somewhat when the window is off center. This is yet another manifestation of the tendency of the AB semblance method to use its larger number of degrees of freedom to find higher semblance values. Stated differently, the AB semblance method has poorer resolving power in time as well as in velocity . The poor resolution in time, however, could be a blessing since, in practice, computation windows generally cannot be expected to be centered on wavelets.

As seen in a comparison of Figures 3, 6 and 7, traditional semblance yields unacceptable estimates of stacking velocity in the presence of polarity reversal, independent of the location of the center of the computation window. The AB semblance measure seems to perform better than does the AK semblance measure in that its peak semblance both has high value and is close to the correct velocity, even when the computation window is not centered on the wavelet.

Test 3: Noise-contaminated data; amplitude variation with offset

We also compared the performances of the three velocity analysis procedures for two other events, one with a positive amplitude gradient and the other with a negative gradient. The first event (Figure 8) has a positive amplitude gradient with offset, with the amplitude doubling from near to far-offset. The signal-to-noise ratio (SNR) measured as the ratio of the amplitude of the event at the center of the offset spread to the root-mean-square

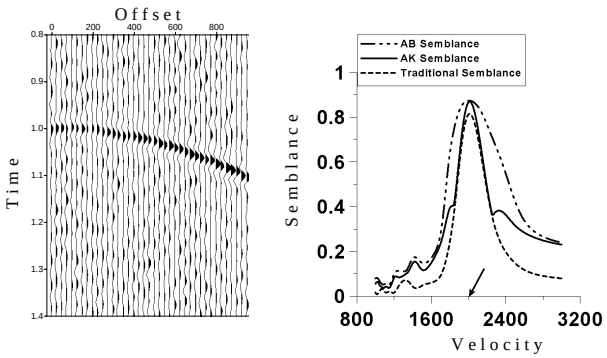

Figure 8. Event with a positive amplitude gradient with offset. The amplitude at far-offset is twice that at near-offset. In this and subsequent figures, units of time are s on the CMP gathers and ms on the semblance plots; units of offset are m; and units of velocity are m/s.

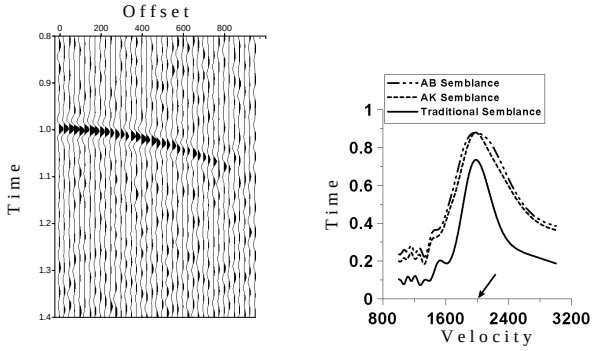

Figure 9. Event with a negative amplitude gradient with offset. The amplitude goes to zero at far-offset.

(rms) amplitude of the background noise is about 2, and the frequency bands of the noise and signal are identical. The semblance curves in this figure were obtained for a window centered on the reflection. The relative performances of the three methods are comparable to those when amplitude is constant with offset (Figure 2), the only difference being a slight reduction in the peak amplitude of the traditional semblance, as one might expect.

Figure 9 shows an event having a negative amplitude

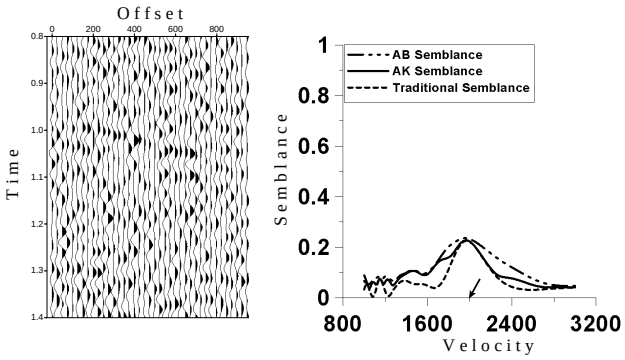

Figure 10. The same event as in Figure 8, but here the signal to noise ratio has been decreased.

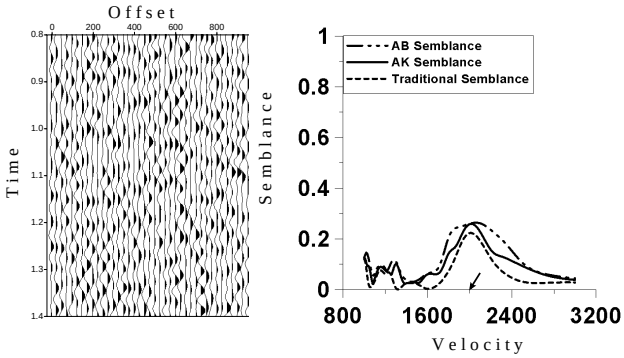

Figure 11. The same event as in Figure 9 but here the signal to noise ratio has been decreased.

gradient with offset, with amplitude decreasing to zero at the far-offset, and the contamination is similar to that in the gather shown in Figure 8. The behavior of the AB and AK semblances is similar: both have high semblance values in comparison to those of the traditional semblance, which, though peaking at the correct velocity has reduced semblance value. For amplitude changes such as those considered here, the velocity that maximizes the semblance is correct for all three methods, but as the amplitude variation increases, the peak value of the traditional semblance decreases. For moderate changes, the traditional semblance may thus serve the purpose acceptably, but for changes that include polarity reversals, amplitude-dependent measures perform better.

Figures 10 and 11 show results for the methods applied to the same two events as in Figures 8 and 9, but now those events are severely contaminated with noise (signal to noise ratio measured as the ratio of the amplitude of the event at the center of the offset spread is approximately the same as the rms amplitude of the background noise). The presence of noise has greatly reduced the peak semblance values, but rather comparably so for all methods. Again, the AB semblance method shows the poorest resolution.

Test 4: Velocity analysis; low noise

In Figures 13, 14 and 15, we compare results of complete velocity analyses based on the three different semblance measures applied to the gather shown in Figure 12. The traditional semblance method produces semblance values less than 0.2 for events with phase reversals and large amplitude variations (note event at 1500 ms); hence, these features are easily missed in the semblance plots. These same events, in contrast, are well represented on the AB and AK semblance panels. For events with negligible amplitude variation, (in particular, the events at times greater than 3000 ms), however, the traditional semblance method produces the best results, due to its

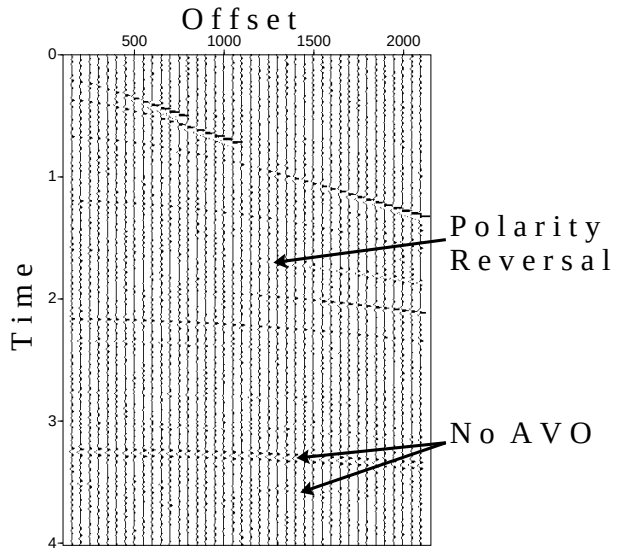

Figure 12. Synthetic CMP gather containing events with polarity reversals, large amplitude variations, and no amplitude variations, in the presence of moderate noise contamination.

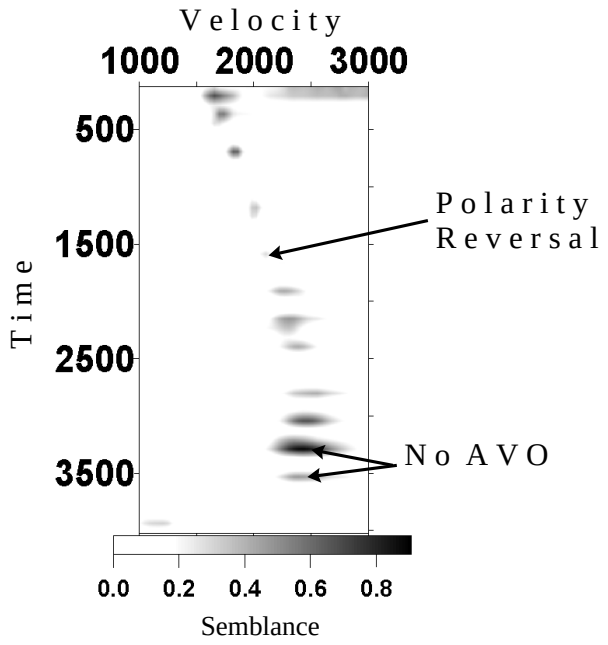

Figure 13. Traditional semblance panel for the gather in Figure 12.

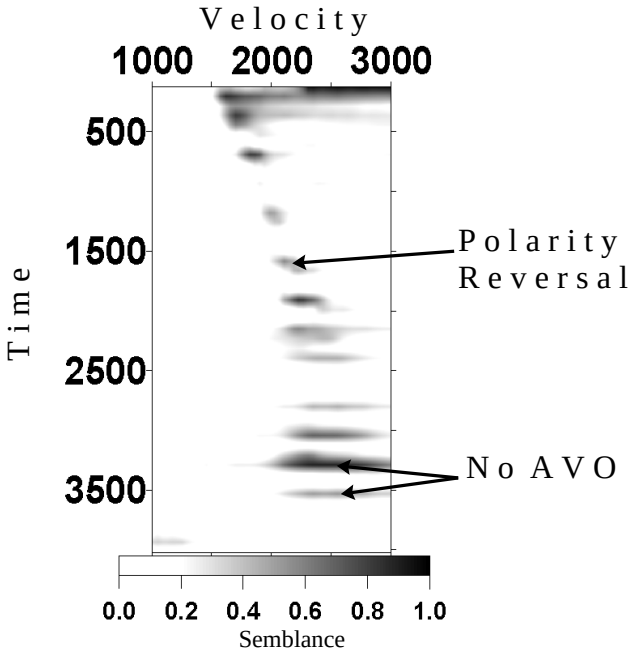

Figure 14. AB semblance panel for the gather in Figure 12.

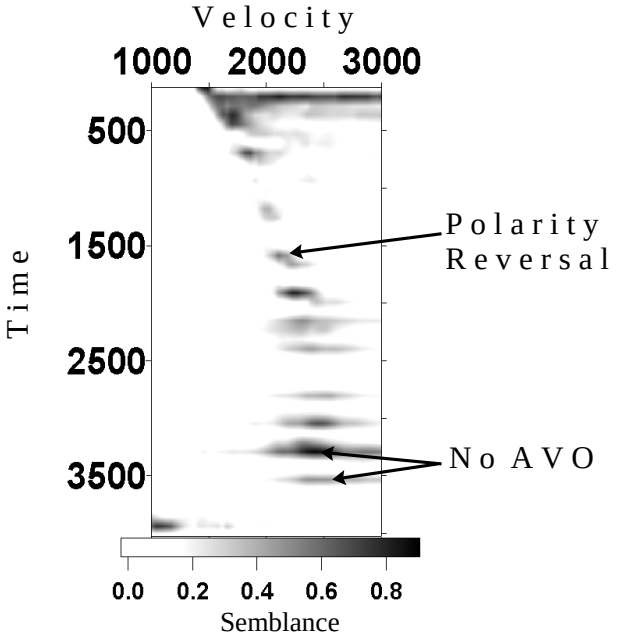

Figure 15. AK semblance panel for the gather in Figure 12.

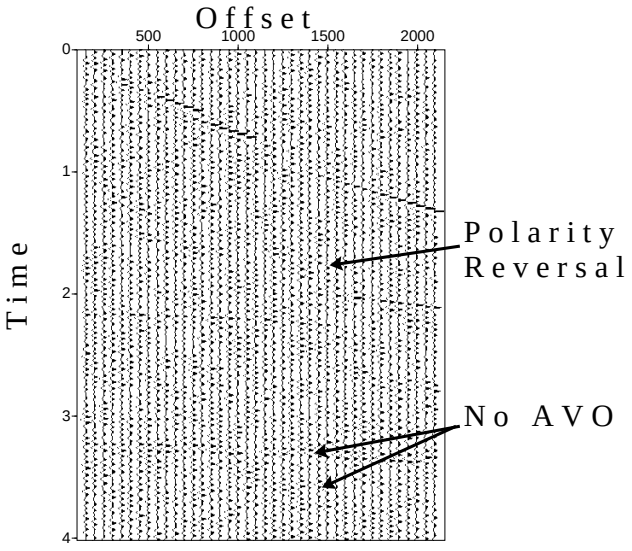

Figure 16. Synthetic CMP gather containing the same events as in Figure 12, but with larger noise contamination.

higher resolution. In such cases, the AB semblance has the poorest velocity resolution, while the AK semblance method performs well for both polarity reversals and for negligible amplitude variation. Its peak is preserved with high semblance values at the correct velocity. In general, events are seen more clearly on the semblance panels for the amplitude-sensitive methods, but they have poorer velocity resolution than in the traditional semblance panels.

Test 5: Velocity analysis; high noise

The CMP gather shown in Figure 16 differs from that in Figure 12 only in that the noise contamination is more severe here. Semblance plots for this CMP gather are shown in Figures 17, 18 and 19. In this set of plots the gray scale starts from a semblance value of 0.1. Traditional semblance fails to even show this small a value for most events. The AB and AK semblance panels show higher semblances and hence preserve the relevant peaks. The improvement can be observed not only for events having polarity reversals but also for events with little amplitude variation. For example, the event just below 2000 ms, having almost no amplitude variation with offset, is hardly visible in the traditional semblance plots. This event, however, is clearly seen in both the AB and AK semblance panels.

Figures 12-19 show that while semblance degrades for all three methods as the level of noise increases, the greater degree of freedom in the amplitude-dependent

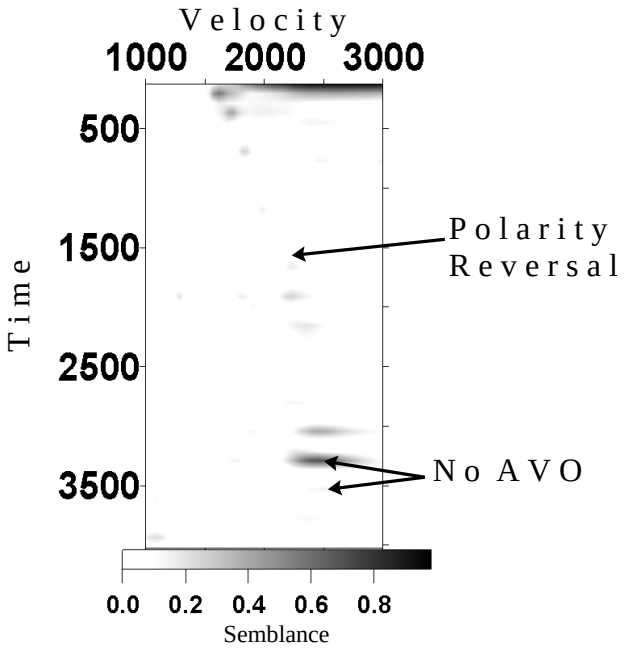

Figure 17. Traditional semblance panel for the gather in Figure 16.

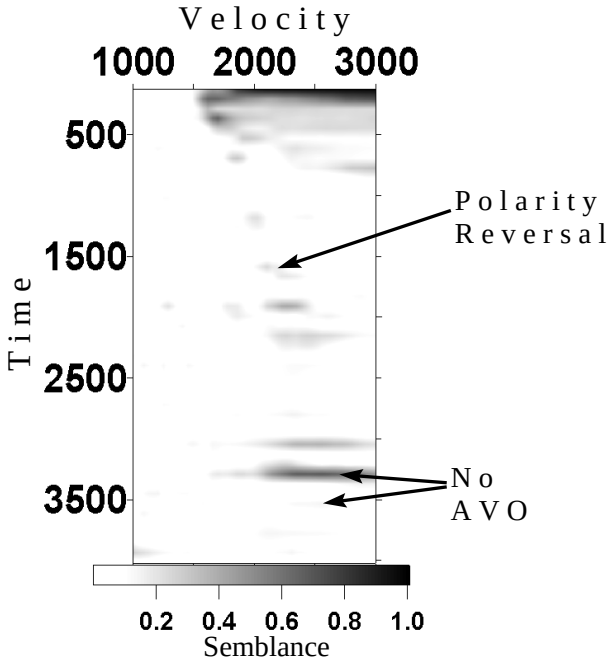

Figure 18. AB semblance panel for the gather in Figure 16.

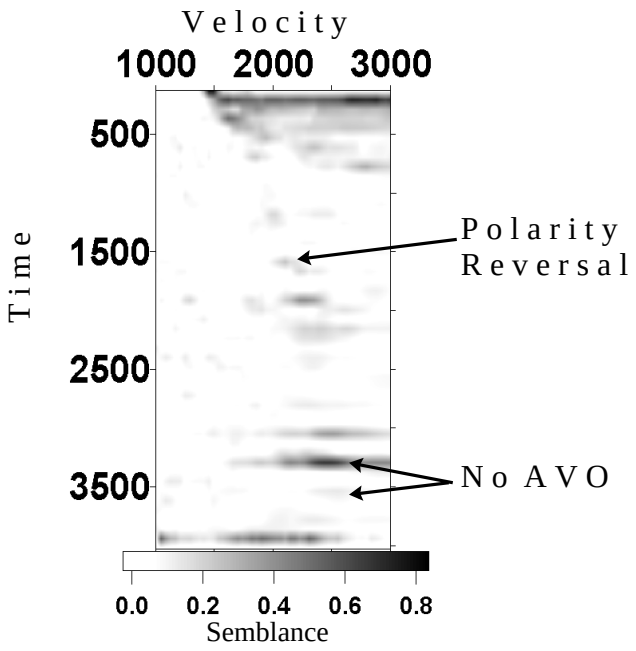

Figure 19. AK semblance panel for the gather in Figure 16.

measures allows for higher semblance values; hence detection of events in the presence of noise is easier with the amplitude-dependent measures. For AB semblance, however, this benefit is achieved at the cost of loss in velocity resolution. The AK method preserves the velocity resolution of traditional semblance for velocities most significant for the analysis (i.e., near semblance peaks) and also remains accurate for events with polarity reversals.

Conclusions and Discussion

Polarity reversals are not common occurrences in CMP gathers, but when they do occur they are of special interest because they may indicate the presence of hydrocarbons. Hence, their detection may be crucial. With the AK method, we follow previous work based on Shuey's (1985) equation, which allows for amplitude variation with offset in the semblance measure. The method uses more fitting parameters than does traditional semblance, but fewer than the number required in AB semblance. In the AK semblance method we have been able to preserve the good points of both traditional semblance and AB Semblance, which requires a regularization term. The pattern of semblance values in Figure 2 is interesting: for an event with little amplitude variation with offset, the AK semblance follows the traditional semblance near the correct velocity, and then jumps to the AB semblance at velocities far from the correct one. This observation may be important for a possible extension of this work to improve semblance measures further.

The amplitude-dependent semblance methods are based on the premise that the amplitude variation inside a semblance window is along a single reflection. Thus we expect these measures to degrade when two or more events overlap within the window. This is also true for traditional semblance. Preliminary test results (not shown here) suggest that the traditional semblance may resolve overlapping events better than will the amplitude-dependent ones.

The computational costs of AK semblance and AB semblance are comparable. Both methods however, are about three times more computationally intensive than is traditional semblance.

Acknowledgements

We thank Phil Anno and Javaid Durrani of Conoco Inc., Ponca City for many helpful suggestions while conducting this study. We thank Conoco Inc. for allowing us to publish these results.

References

Biondi, B.L., and Kostov, C., 1989, High resolution velocity spectra using eigenstructure methods: Geophysics, 54, 832-842.

Corcoran,C.T., 1989, Method of processing seismic data, European Patents 89200724.6.

Key, S.C. and Smithson,S.B., 1990, New approach to seismic-reflection event detection and velocity determination: Geophysics, 55, 1057-1069.

Menke, W., 1984, Geophysical data analysis: discrete inverse theory: Academic Press Inc.

Sarkar, D, 1999, AVO and velocity analysis in an isotropic layered earth, MS Thesis, University of Oklahoma.

Sarkar, D., Lamb, W. and Castagna, J.P., 1999, AVO and velocity analysis: 69th Ann. Internat. Mtg., Soc. Expl. Geophys., Expanded Abstracts, 840-843.

Shuey, R.T., 1985, A simplification of the Zoeppritz equations, Geophysics, 50, 609-614.

Symes,W.W. and Kern, M., 1994, Inversion of reflection seismograms by the differential semblance analysis: Algorithm structure and synthetic examples: Geophysical Prospecting, 42, 565-614.

Taner, M.T., and Koehler. T., 1969, Velocity spectra: Digital computer derivation and applications of velocity functions. Geophysics, 34: 859-881.